

Multiscale Bessel beams generated by a tunable acoustic gradient index of refraction lens

Euan McLeod, Adam B. Hopkins, and Craig B. Arnold

Department of Mechanical & Aerospace Engineering, Princeton University, Princeton, New Jersey 08544

Received June 12, 2006; revised August 7, 2006; accepted August 9, 2006;
posted August 15, 2006 (Doc. ID 71925); published October 11, 2006

A beam that resembles a Bessel beam on two scales is generated using a tunable acoustic gradient index of refraction (TAG) lens. The minor scale of the TAG-generated Bessel beam is nondiffracting and self-healing. The major scale of the beam diffracts while still forming a Bessel pattern due to the specific geometry of the TAG lens. The acoustic and optical theory behind the TAG lens is outlined, and the experimental beam itself is presented. The major and minor rings are explained, and the TAG beam is compared with both axicon-generated and conventionally focused Gaussian beams. © 2006 Optical Society of America

OCIS codes: 230.1040, 110.2760, 140.3300, 070.1060, 160.1050.

The study of Bessel beams has been a topic of some interest over the past two decades.^{1–3} Much of this interest has centered around the beams' two exceptional qualities: they maintain a narrow beam width over a long propagation distance (termed "nondiffracting"), and they can reconstruct themselves around obstacles (termed "self-healing"). Based on these properties, many different uses for Bessel beams have been proposed, including optical manipulation,^{4–7} nonlinear optics,^{8–11} and metrology.^{12,13}

The use of acousto-optic modulators for diverting a beam has become standard practice in optics, and the use of acoustic waves in fluids to create beams with concentric ring patterns has been noted.^{14,15} However, to our knowledge the creation of multiscale Bessel beams by lenses has not previously been demonstrated. Typically, conventional Bessel beams are created by using spatial light modulators or fixed optical elements. This Letter will present the generation of a tunable Bessel beam by use of a dynamic optical element and provide a model to explain the two scales of the observed Bessel beam. In contrast with traditional approaches, this lens enables the combination of tunability with high switching speeds and high damage thresholds.

The output pattern can be seen in Fig. 1, where each bright major ring of the beam is surrounded by several dimmer minor rings. On the minor scale, the beam is nondiffracting and approximates an axicon-generated beam, and it can therefore be considered a Bessel beam. On the major scale, the beam forms a circular pattern similar to a Bessel beam, where each ring contains its own minor Bessel pattern. We call the device used to create these beams a tunable acoustic gradient index of refraction (TAG) lens.

The TAG lens is a cylindrical cavity filled with a refractive material where acoustically driven fluctuations in density result in gradients in refractive index. The cavity is bounded by a circular piezoelectric ring and two flat glass windows (see Fig. 2). One would typically use a low-viscosity liquid; however, multiphase systems¹⁵ and pure solids and gases may also be used. The piezoelectric is driven by an AC sig-

nal that excites cylindrical modes in the form of pressure waves within the lens.

The TAG lens in this study has an inner diameter of 7.1 cm and a length of 3.6 cm. The fluids used are 5 and 0.65 cS Dow Corning 200 Fluids (silicone oil), which have indices of refraction of 1.3960 and 1.375, respectively, under standard conditions. The TAG lens is driven by a function generator (Stanford Research Systems, DS345) passed through a RF amplifier (T&C Power Conversion, AG 1006). This setup was used to radially drive the piezoelectric with AC voltages in the range of 40–100 V_{pp} at frequencies between 100 and 500 kHz. Lasers at 532 nm and, where noted, 650 nm, were used to study the lens. The resulting intensity patterns produced by the lens are then sampled at various distances by use of a CCD camera (Cohu 2622 and Diagnostic Instruments Color Mosaic).

The basis behind the operation of the lens is that the piezoelectric generates standing sound waves that induce density variations, which are correlated with index of refraction variations. Assuming that the radial wall of the chamber vibrates sinusoidally

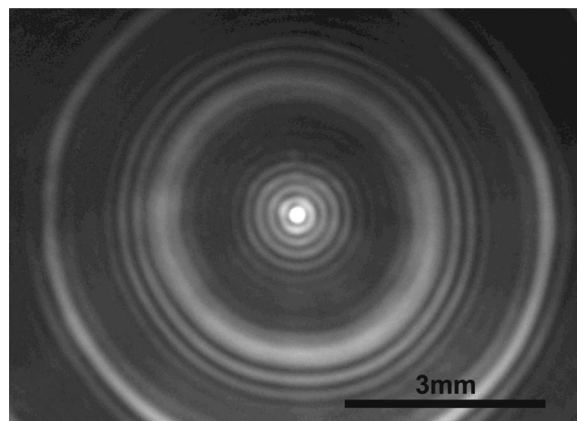


Fig. 1. Experimental major and minor rings of the multiscale Bessel beam created by the TAG lens. The beam is imaged at a distance of 80 cm behind the back face of the lens. The TAG lens is driven at 257.0 kHz and 74.4 V_{pp} . There are two major rings visible here.

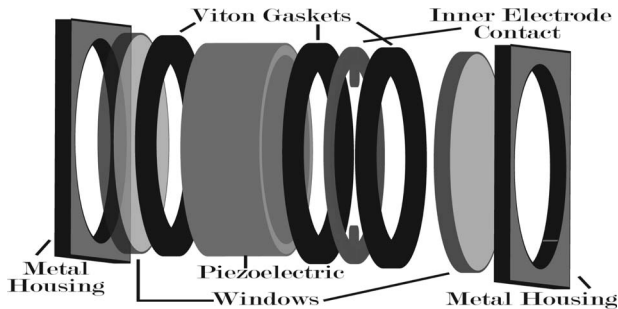


Fig. 2. Cross-section of the TAG lens showing its assembly.

in time with frequency ω_f , the linearized, inviscid, cylindrically symmetric solution for the index of refraction in the cavity is given by¹⁶

$$n(r, t) = n_0 + n_A J_0\left(\frac{\omega_f r}{v}\right) \sin(\omega_f t), \quad (1)$$

where n_0 is the mean index of refraction of the material and v is the speed of sound. In Eq. (1), n_A depends on many parameters, including the mean index, mean density, speed of sound, driving voltage amplitude, driving frequency, and lens size. Observed and theoretical values for n_A were of the order of 10^{-5} .

By using Fourier methods, it is possible to compute the image intensity pattern at any distance resulting from the transmission of light through a lens with the above time-dependent index of refraction. The formulation below assumes an optically thin lens through which light propagates in the positive z direction. (x_0, y_0) are coordinates at the lens plane, and $(x_{\text{img}}, y_{\text{img}})$ are coordinates at the image plane. The Rayleigh–Sommerfeld integral then yields the intensity pattern:

$$I(x_{\text{img}}, y_{\text{img}}, t) = \frac{z^2}{2\lambda_0^2} \sqrt{\frac{\epsilon_0}{\mu_0}} \left| \iint U_0(x_0, y_0) \times \frac{e^{ik_0[d+n(x_0, y_0, t)L]}}{d^2} dx_0 dy_0 \right|^2, \quad (2)$$

where the integration is performed over the aperture of the TAG lens. λ_0 is the free-space wavelength of the light; ϵ_0 and μ_0 are the free-space permittivity and permeability, respectively; k_0 is the free-space propagation constant ($2\pi/\lambda$); L is the length of the lens; and

$$d = [z^2 + (x_{\text{img}} - x_0)^2 + (y_{\text{img}} - y_0)^2]^{1/2} \quad (3)$$

is the distance from a point on the lens plane to a point on the image plane. The time dependence of the incident laser beam's electric field is neglected because we consider only output intensity and because the lens is driven at frequencies much lower than the frequency of the laser light (10^5 versus 10^{14} Hz).

Looking at the image of a TAG beam (Fig. 1), one notices two sets of rings: a set of bright major rings with a large space between them and a set of dimmer minor rings surrounding each major ring and the

central spot. These are the two scales of the multi-scale TAG-generated Bessel beam. This experimentally observed pattern can be theoretically generated by time averaging the intensity given by Eq. (2), assuming the index of refraction is of the form in Eq. (1).

First, to explain the major rings, consider Eq. (1). In a gradient index lens, light is deflected toward the greater index of refraction, therefore at any instant in time we expect bright zones with spatial periodicity of the peaks of $J_0(\omega_f r/v)$. However, each half-cycle the index profile will be inverted and the valleys will become peaks. So the time-average intensity pattern should have the same spatial periodicity as the peaks of $J_0^2(\omega_f r/v)$. The observed spatial periodicity of the major scale pattern is consistent with that predicted here by the linear theory. In Fig. 3, the theoretical first major ring occurs at the same location as the experimental ring. This holds for the subsequent major rings (not pictured). Previous attempts to explain this pattern invoked nonlinear effects to predict a spatial variation in time-average refractive index.¹⁵ However, in predicting time-average image intensity, these effects are negligible compared with the linear effects.

To explain the minor rings, first consider the index of refraction at one instant in time. If a peak in this index of refraction profile was replaced by a linear approximation, then the radial gradient in the index of refraction would be constant and that peak would be fundamentally equivalent to an axicon lens. This is the source of the nondiffracting and self-healing properties of the minor scale Bessel beam.

Under operation, the central index will continuously vary from positive to negative, creating a Bessel pattern that changes in time, and we observe the time-average intensity pattern (see Fig. 3). Note that the locations of the minor rings is consistent with the beam generated by an axicon with an effective cone angle of 179.556° . For many applications, cone angles close to 180° are used because of their

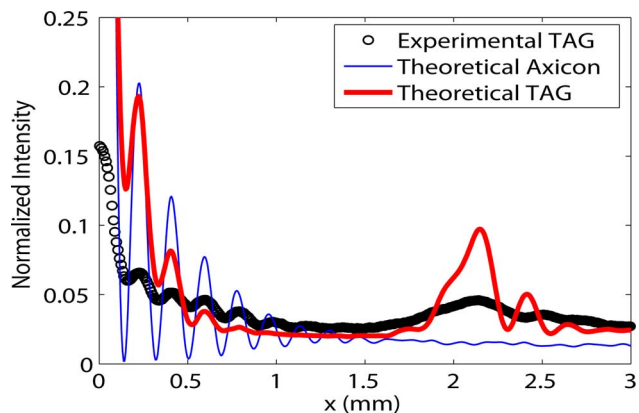


Fig. 3. (Color online) Comparison between theoretical and experimental TAG beam and a simulated axicon. The experimental data are taken from Fig. 1, and the model uses $n_A = 4.4 \times 10^{-5}$. In these units, the theoretical TAG has a peak intensity of 1, and the axicon has a peak intensity of 1.32. The beams have been normalized to have equal power within a radius of 1.5 mm, the approximate limit of the central TAG minor scale Bessel beam.

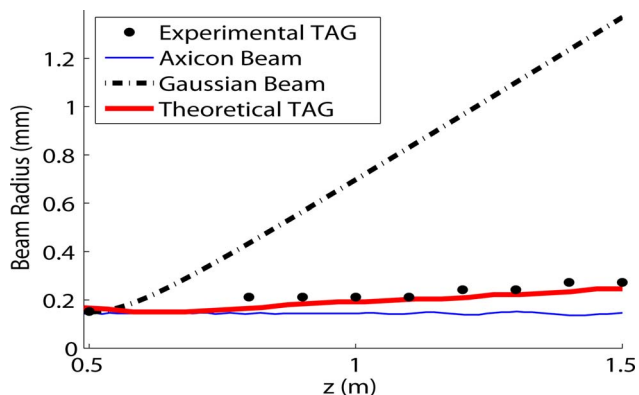


Fig. 4. (Color online) Radial coordinate of the first local intensity minimum. For the Gaussian beam, the beam radius is the $1/e$ radius. The laser wavelength used here is 650 nm, and the TAG lens is driven at $74.4 V_{pp}$ at 265.7 kHz. The axicon has a cone angle of 179.50° , and the simulated TAG beam uses $n_A = 5.5 \times 10^{-5}$.

long working distance and large ring spacing.⁴ The intensity cascade observed in the experimental data is caused by the time averaging and is predicted by the linear theory.

To justify that the TAG beam can be considered diffractionless over a range, its central spot divergence is compared via experiment and simulation with the divergence of both a Gaussian beam and an axicon-generated Bessel beam in Fig. 4. The Gaussian beam is constructed to have a maximum intensity approximately 50 cm from the lens and to have a $1/e$ beam waist of $150 \mu\text{m}$ there to match the central spot size of the experimental TAG beam. Both the axicon and TAG beam simulations include an aperture 8 mm in diameter just before the lens. From the figure, we can see that the axicon and TAG beams have comparable divergences much smaller than the divergence of the Gaussian beam. Therefore, the TAG beam can be considered diffractionless on the minor scale, and its properties are well predicted by the theory behind the lens.

The major scale rings are fundamentally different from the minor scale diffractionless rings in that their location is not determined by the amplitude of the gradient in the refractive index, but rather purely by the location of the antinodes in the index. However, the amplitude is important in establishing the minor rings around each major ring, leading to the diffractionless multiscale behavior.

One especially attractive feature of the TAG lens is its tunability via driving voltage frequency and amplitude, indicated by the dependence of refractive index on the driving parameters. By varying these parameters, it is possible to independently tune the major and minor scales of the beam. Modifying the

driving voltage alters the ring spacing of the beam, effectively adjusting the cone angle of the equivalent axicon. For example, adjusting the ring spacing can provide a simple method to manipulate particles that are optically trapped in the beam. In addition, the long diffractionless line focus of a Bessel beam can be useful for high-aspect-ratio material modifications. The TAG lens can be tuned to adjust the diameter, length, and working distance of this line focus. SLMs also enable tunability, but the TAG lens has the potential for higher switching speeds that are limited only by the speed of sound and viscosity in the liquid, and high damage thresholds due to low absorption in the replaceable liquid refracting medium.

Finally, the concept of a TAG lens is not restricted to cylindrical geometries. For example, a rectangular geometry would lead to the creation of a rectangular lattice of Bessel beams, which could be useful in particle sorting and material patterning applications.

We thank Ed Rietman for introducing us to the idea of an acoustic lens, and Mikko Haataja, Jason Fleischer, and Clancy Rowley for useful discussions. E. McLeod's e-mail address is emcleod@princeton.edu.

References

1. J. Durnin, *J. Opt. Soc. Am. A* **4**, 651 (1987).
2. Z. Bouchal, *Czech. J. Phys.* **53**, 537 (2003).
3. D. McGloin and K. Dholakia, *Contemp. Phys.* **46**, 15 (2005).
4. J. Arlt, V. Garcés-Chávez, W. Sibbett, and K. Dholakia, *Opt. Commun.* **197**, 239 (2001).
5. V. Garcés-Chávez, K. Volke-Sepulveda, S. Chávez-Cerda, W. Sibbett, and K. Dholakia, *Phys. Rev. A* **66**, 063402 (2002).
6. V. A. Soifer, V. V. Kotlyar, and S. N. Khonina, *Phys. Part. Nucl.* **35**, 733 (2004).
7. T. Čížmár, V. Garcés-Chávez, K. Dholakia, and P. Zemánek, *Appl. Phys. Lett.* **86**, 174101 (2005).
8. T. Wulle and S. Herminghaus, *Phys. Rev. Lett.* **70**, 1401 (1993).
9. S. P. Tewari, H. Huang, and R. W. Boyd, *Phys. Rev. A* **54**, 2314 (1996).
10. L. Niggli and M. Maier, *Opt. Lett.* **22**, 910 (1997).
11. J. Arlt, K. Dholakia, L. Allen, and M. J. Padgett, *Phys. Rev. A* **60**, 2438 (1999).
12. T. Aruga, S. W. Li, S. Yoshikado, M. Takabe, and R. Li, *Appl. Opt.* **38**, 3152 (1999).
13. K. Wang, L. Zeng, and C. Yin, *Opt. Commun.* **216**, 99 (2003).
14. K. A. Higginson, M. A. Costolo, and E. A. Rietman, *Appl. Phys. Lett.* **84**, 843 (2004).
15. K. A. Higginson, M. A. Costolo, and E. A. Rietman, *J. Appl. Phys.* **95**, 5896 (2004).
16. E. McLeod and C. B. Arnold, "Mechanics and refractive power optimization of tunable acoustic gradient index lenses," in preparation.